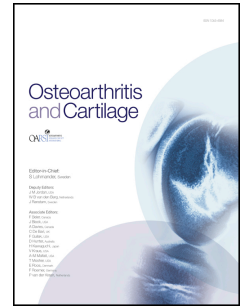


Journal Pre-proof

Osteoarthritis-related nociceptive behaviour following mechanical joint loading correlates with cartilage damage

F. ter Heegde, A.P. Luiz, S. Santana-Varela, R. Magnusdottir, M. Hopkinson, Y. Chang, B. Poulet, R.C. Fowkes, J.N.Wood, C. Chenu



PII: S1063-4584(19)31300-7

DOI: <https://doi.org/10.1016/j.joca.2019.12.004>

Reference: YJOCA 4570

To appear in: *Osteoarthritis and Cartilage*

Received Date: 18 July 2019

Revised Date: 18 December 2019

Accepted Date: 22 December 2019

Please cite this article as: Heegde Ft, Luiz AP, Santana-Varela S, Magnusdottir R, Hopkinson M, Chang Y, Poulet B, Fowkes RC, J.N.Wood Chenu C, Osteoarthritis-related nociceptive behaviour following mechanical joint loading correlates with cartilage damage, *Osteoarthritis and Cartilage*, <https://doi.org/10.1016/j.joca.2019.12.004>.

This is a PDF file of an article that has undergone enhancements after acceptance, such as the addition of a cover page and metadata, and formatting for readability, but it is not yet the definitive version of record. This version will undergo additional copyediting, typesetting and review before it is published in its final form, but we are providing this version to give early visibility of the article. Please note that, during the production process, errors may be discovered which could affect the content, and all legal disclaimers that apply to the journal pertain.

© 2019 Published by Elsevier Ltd on behalf of Osteoarthritis Research Society International.

1 Osteoarthritis-related nociceptive behaviour following
2 mechanical joint loading correlates with cartilage
3 damage

4
5 F. ter Heegde^{1,2}, A.P. Luiz², S. Santana-Varela², R. Magnusdottir¹, M. Hopkinson¹, Y. Chang³, B.
6 Poulet⁴, R.C. Fowkes⁵, J.N.Wood², C. Chenu¹

7
8 ¹Skeletal Biology Group, Comparative Biomedical Science, Royal Veterinary College, London NW1
9 0TU, UK

10 ²Molecular Nociception Group, Wolfson Institute for Biomedical Research, University College
11 London, London WC1E 6BT UK

12 ³Research Office, Royal Veterinary College, London NW1 0TU, UK

13 ⁴Musculoskeletal Biology, Institute of Ageing and Chronic Disease, University of Liverpool, Liverpool
14 L69 3BX, UK

15 ⁵Endocrine Signalling Group, Comparative Biomedical Science, Royal Veterinary College, London
16 NW1 0TU, UK

17
18 Contact details:

19 F. ter Heegde (freijaterheegde@gmail.com), A.P. Luiz (a.luiz@ucl.ac.uk), S. Santana-Varela
20 (s.santana@ucl.ac.uk), R. Magnusdottir (rmagnusdottir@rvc.ac.uk), M. Hopkins
21 (mhopkinson@rvc.ac.uk), Y. Chang (ychang@rvc.ac.uk), B. Poulet (b.poulet@liverpool.ac.uk), R.C.
22 Fowkes (rfowkes@rvc.ac.uk), J.N.Wood (j.wood@ucl.ac.uk), C. Chenu (cchenu@rvc.ac.uk)

23
24 Corresponding author:

25 Chantal Chenu

26 The Royal Veterinary College

27 Royal College Street

28 London

29 NW1 0TU

30 United Kingdom

31 +44 (0)20 74685045

32 cchenu@rvc.ac.uk

33
34 Running title: MJL-induced pain and cartilage damage

Abstract

36

37 **Objective:** In osteoarthritis (OA), the pain-structure relationship remains complex and poorly
38 understood. Here, we used the mechanical joint loading (MJL) model of OA to investigate both knee
39 pathology and nociceptive behaviour.

40

41 **Design:** MJL was used to induce OA in the right knees of 12-week-old male C57BL/6 mice (40
42 cycles, 9N, 3x/week for two weeks). Mechanical sensitivity thresholds and weight-bearing ratios were
43 measured before loading and at weeks one, three and six post-loading. At these time points, separate
44 groups of loaded and non-loaded mice ($n=12/\text{group}$) were sacrificed, joints collected, and fur
45 corticosterone levels measured. μCT analyses of subchondral bone integrity was performed before
46 joint sections were prepared for nerve quantification, cartilage or synovium grading (scoring system
47 from 0-6).

48

49 **Results:** Loaded mice showed increased mechanical hypersensitivity paired with altered weight-
50 bearing. Initial ipsilateral cartilage lesions one-week post-loading (1.8 ± 0.4) had worsened at weeks
51 three (3.0 ± 0.6 , $CI=-1.8--0.6$) and six (2.8 ± 0.4 , $CI=-1.6--0.4$). This increase in lesion severity
52 correlated with mechanical hypersensitivity development (correlation; 0.729 , $p=0.0071$). Loaded mice
53 displayed increased synovitis (3.6 ± 0.5) compared to non-loaded mice (1.5 ± 0.5 , $CI=-2.2--0.3$) one-
54 week post-loading which returned to normal by weeks three and six. Similarly, corticosterone levels
55 were only increased at week one post-loading ($0.21\pm 0.04\text{ng/mg}$) compared to non-loaded controls
56 ($0.14\pm 0.01\text{ng/mg}$, $CI=-1.8--0.1$). Subchondral bone integrity and nerve volume remained unchanged.

57

58 **Conclusions:** Our data indicates that although the loading induces an initial stress reaction and local
59 inflammation, these processes are not directly responsible for the nociceptive phenotype observed.
60 Instead, MJL-induced allodynia is mainly associated with OA-like progression of cartilage lesions.

61

62

63

64 **Key words:** Osteoarthritic pain, cartilage lesions, synovitis, knee innervation, bone integrity, stress

1 Introduction

2

3 Osteoarthritis is typically recognized as a degenerative joint disease characterized by a loss of
4 cartilage. Although much of the aetiology remains unknown, the approach to understanding OA has
5 evolved from being cartilage focussed to a more multifactorial, whole joint view of the disease [1].
6 The identification of pathologies in multiple joint tissues and their subsequent involvement in OA, has
7 brought up the question how these pathologies contribute to the clinical presentation of OA-associated
8 pain. For the patients, it is this clinical presentation of pain that is the most problematic symptom of
9 OA. Despite the importance of pain as a symptom of knee OA, much remains unclear about how knee
10 pathology is associated with pain in OA [2].

11

12 The complexity of this structure-pain relationship is highlighted by epidemiological studies presenting
13 conflicting results on the correlation between pain severity and MRI or radiograph read-outs of tissue
14 damage. Whilst some clinical studies have shown positive correlations between pain and a variety of
15 knee pathologies including bone marrow lesions [3-7], synovitis [3, 8], effusion [4, 8, 9], cartilage
16 degradation [6, 10-12] and meniscal tears [3], other studies show a negative or neutral correlation
17 between pain and bone marrow lesions [9, 10], synovitis [13, 14], cartilage damage [9] or meniscal
18 pathology [9, 10, 15, 16]. Evidently, there is currently no consensus on which single tissue pathology
19 or combination of pathologies drives OA-associated pain. Furthermore, it is likely that the magnitude
20 of contribution to pain severity for each tissue pathology is dependent on the stage and progression of
21 the disease. This is then further complicated by patient-specific factors such as genetics, age and sex
22 which, in part, can explain the discordance in patient association studies.

23

24 Animal models of OA, such as the MJL, can be used to address temporal questions regarding the
25 development of knee pathology in correlation to OA-associated pain. Mechanical loading of the knee
26 joint is a novel, non-invasive murine model of OA. This model induces OA by intermittent, repetitive
27 loading of the tibia through the knee and ankle joints. Originally, this model has been used to
28 investigate the osteogenic effect of mechanical loading on the tibia [17]. Poulet and colleagues [18]
29 were the first to investigate the effects of different loading regimes on the knee joint. Mice sacrificed
30 directly after two weeks of loading at 9N showed cartilage damage, osteophyte formation and
31 meniscus pathologies combined with a thickening and fibrosis of the synovium indicative of
32 inflammation. When mice were loaded at 9N for two weeks and sacrificed three weeks later, knee
33 pathology analysis showed increased cartilage damage and meniscal pathology whilst the osteophyte
34 formation remained the same and signs of synovial inflammation had decreased. Subchondral bone
35 thickening and increased trabecular bone percentage were only seen in mice loaded at 9N for five
36 consecutive weeks [19]. This initial characterization of the knee pathology following loading provided

37 the first evidence that the MJL model could be used to study OA initiation and progression in a
38 controlled, non-invasive manner.

39

40 In previous work, we showed that the mechanical joint loading model at 9N induces a progressive and
41 chronic pain phenotype from two weeks post-loading, characterized by the development of ipsilateral
42 mechanical hypersensitivity, altered weight bearing and reduced mobility, without affecting thermal
43 sensitivity [20]. Here, we used this model to gain insight into how the development of OA pathology
44 in different tissues relates to the development of MJL-induced allodynia [20]. To this end, knee joint
45 pathology, pain severity and animal welfare were assessed at weeks one, three and six post-loading.
46 Pain severity was determined as the nociceptive response to von Frey hairs, taken as a measure for
47 mechanical allodynia, and by measuring hindlimb weight bearing wherein a reduced weight borne on
48 the ipsilateral hindlimb is indicative of increased sensitivity [21, 22]. It should be noted that, although
49 these parameters are routinely used for assessing nociception in murine OA-related pain models [23-
50 25], they are measurements of referred knee pain rather than being specific for knee nociception.
51 Alongside behavioural measurements to evaluate pain, a total of five markers were measured at these
52 time points to track the OA development; the severity of cartilage damage and synovitis in both
53 ipsilateral and contralateral knees, the volume of sympathetic and sensory nerve fibres present in the
54 ipsilateral knee, the integrity of the subchondral bone in the ipsilateral knee and the corticosterone
55 levels in the fur as a measure for chronic stress. These read-outs of OA progression were subsequently
56 correlated to behavioural read-outs to determine which pathologies matched the MJL-induced pain
57 phenotype.

58 Method

59

60 Naïve, male 10-week-old C57bl/6 mice (Charles River, Oxford, UK) were housed in groups of four in
61 individually ventilated cages and fed a standard RM1 maintenance diet *ad libitum*. All experiments
62 were carried out in compliance with the Animals (Scientific Procedures) Act (1986) and approved by
63 the College's Ethics and Welfare Committee and UK Home Office.

64

65 Osteoarthritis was induced in the right knee of 12-week-old mice by a two-week loading regime using
66 an electronic testing machine (Bose 3100; TA instruments), as described previously [18, 20]. Briefly,
67 the tibia was positioned vertically between two custom-made cups to fixate the knee and ankle joint in
68 deep flexion of 45°. Axial compressive loads were applied to the knee joint via the upper loading cup
69 controlled by software delivered by the loading system (WinTest7 Bose). One loading cycle consisted
70 of 9.9 seconds holding time with a load magnitude of 2N after which a peak load of 9N was applied
71 for 0.05sec. This 10 second trapezoidal wave loading cycle is repeated 40 times within one loading
72 episode. These loading episodes were applied three times per week, performed on alternating days, for
73 two consecutive weeks. The left hindlimb was left unloaded. No other experiments were performed
74 on the mice during the two weeks of loading.

75

76 Osteoarthritis was induced in a total of 36 mice. Another 36 cage- and age-matched mice did not
77 undergo loading but were subjected to anaesthesia and served as the non-loaded controls. Separate
78 groups of loaded mice and non-loaded controls were sacrificed at one-, three- and six-weeks post-
79 loading to conduct post-mortem analysis ($n=2$ per condition and time point). Behaviour was measured
80 before loading (week -3) after which development of nociception was verified at weeks one, three and
81 six post-loading, a day before the sacrifice time-point. Behavioural analysis conducted included von
82 Frey measurements in both hindlimbs to measure mechanical sensitivity thresholds and weight
83 bearing to measure asymmetry in stance. Researchers performing behavioural testing were blinded to
84 the condition of the mice.

85

86 At each time point, post-mortem samples were collected for analysis. Half of the samples were used
87 for μ CT analysis, OA and synovitis grading ($n=6$ /group) whilst the other half were used for nerve
88 analysis ($n=6$ /group). Hindlimbs used for μ CT analysis, synovitis and OA grading were collected
89 directly after sacrifice, post-fixed (4% formalin) and stored at 4°C. These samples were first scanned
90 using the μ CT after which they were processed for paraffin embedding and grading. Cartilage
91 integrity was scored using the Osteoarthritis Research Society International grading system (range 0–
92 6) [26] whilst synovitis was scored using the six-point grading system as described by Lewis and
93 colleagues [27]. Hindlimbs collected for nerve analysis were perfused (12,5% picric acid, 4%
94 formalin fixative) dissected out on ice, post-fixed, decalcified and then stored in sucrose solution at -

95 20°C [28]. Immunocytochemistry was used to identify sensory and sympathetic nerves [29] using
96 primary antibodies against calcitonin gene-related peptide (CGRP) and tyrosine hydroxylase (TH),
97 respectively. Finally, the fur was collected from all animals to analyse the corticosterone levels as a
98 measure for chronic stress.

99

100 Extended methods for both the behavioural measurements and the post-mortem analysis can be found
101 in the supplementary methods.

102

103 Data were analysed using GraphPad Prism (7.04). Results are presented as mean±SD. Mice were
104 assigned conditions in a pseudo-random order, ensuring comparable behavioural baseline values and
105 allocating different conditions within the home cage. Repeated behavioural measurements were
106 analysed using a repeated two-way ANOVA. OA pathology read-outs for loaded and non-loaded
107 groups across time points were compared using a parametric two-way ANOVA. Homogeneity of
108 variances was assessed using Levene's test. Normality of the residuals were evaluated by visual
109 inspection of the histograms. In the case of a significant time, group or interaction effect, analysis was
110 performed to identify which data points showed differences. Between group differences at specific
111 time points or within group differences between time points are presented with the corresponding
112 95% confidence interval (CI) of the difference. The Spearman's rank correlation between multiple
113 behavioural and OA pathology read-outs was calculated using R (version 5.3.1), with results
114 presented as a heatmap. Spearman's correlation coefficients and the corresponding p-values between
115 parameters can be found in supplementary data. For each time point, the difference between baseline
116 and final behavioural thresholds (difference score) of the ipsilateral mechanical thresholds and weight
117 bearing values were used. Parameters used as measures for knee pathology are all ipsilateral values.
118 Parameters showing the clearest pattern in correlation with behaviour over time were plotted
119 independently to visualize the progression of the behavioural parameter in relation to the knee
120 pathology. Additionally, linear model was employed to evaluate the association between behaviours
121 and OA pathology over time (behaviours, time, and their interaction in the model).

122 Results

123

124 Mice loaded at 9N developed mechanical hypersensitivity in both hindlimbs and an altered weight
125 bearing (Fig.1). Mice sacrificed at weeks three (Fig.1B) and six (Fig.1C) showed a difference in
126 ipsilateral mechanical threshold values between loaded mice and non-loaded controls. Non-loaded
127 controls showed an initial drop in threshold values at week one but then recovered whilst threshold
128 values in loaded mice further decreased at weeks three ($0.175\text{g}\pm 0.0.7\text{g}$, $CI=0.26-0.67$) and six
129 ($0.140\text{g}\pm 0.16\text{g}$, $CI=0.30-0.71$) post-loading compared to baseline values ($0.645\text{g}\pm 0.29\text{g}$).
130 Contralateral mechanical hypersensitivity development was less pronounced with loaded mice
131 showing a lower threshold level ($0.205\text{g}\pm 0.17\text{g}$) compared to non-loaded mice ($0.571\text{g}\pm 0.22\text{g}$,
132 $CI=0.14-0.59$) only six weeks post-loading (Fig.1F). Alteration in weight bearing occurred alongside
133 this development of mechanical hypersensitivity. Loaded mice sacrificed at weeks one (Fig.1G), three
134 (Fig.1H) and six (Fig.1I) post-loading showed a significant alteration in weight bearing over time. At
135 six weeks post-loading the difference in weight borne on the ipsilateral paw between loaded
136 ($44.13\%\pm 3.8\%$) and non-loaded ($49.95\%\pm 5.4\%$, $CI=1.80-9.93$) mice was most pronounced. See
137 supplementary Fig1 for individual behavioural values.

138

139 Following MJL, both knees showed signs of cartilage damage; in the ipsilateral knee, MJL induced
140 mild cartilage lesions which progressively worsened over time whilst the contralateral knees of loaded
141 mice showed cartilage damage of a lesser extent and only at six weeks post-loading (Fig.2). Non-
142 loaded, naïve mice did not show any change in cartilage integrity over time in either knee. In the first
143 week following MJL the maximum OA score (Fig.2A) in the ipsilateral knees of loaded mice
144 (1.8 ± 0.4) was higher compared to non-loaded controls (0.9 ± 0.4 , $CI=-1.45--0.31$). The lesions
145 worsened up till three weeks post-loading (3.0 ± 0.3) after which they stabilized at six weeks post-
146 loading (2.8 ± 0.2). Summed OA scores of the ipsilateral knees (Fig.2C) show a similar advancement
147 of OA severity with lesions progressing from week one (11.0 ± 6.5) to three (31.3 ± 9.0 , $CI=-30.75--$
148 9.75) and stabilizing at week six (37.1 ± 7.9 , $CI=-36.58--15.59$). Contralateral lesions develop at a later
149 stage with maximum OA scores (Fig.2B) of loaded mice (1.8 ± 0.7) being higher than non-loaded mice
150 (1.0 ± 0.0 , $CI=-1.55--0.12$) at six weeks post-loading. Summed OA scores (Fig.2D) show a more
151 progressive increase of lesions in the contralateral knees of loaded mice with values steadily
152 increasing from week one (5.8 ± 5.8) to three (13.8 ± 4.6) and six (22.0 ± 9.7) post-loading.

153

154 The synovial lining of loaded mice showed increased signs of inflammation compared to non-loaded
155 controls in the first weeks following MJL (Fig.3). Maximum synovitis scores for the ipsilateral knees
156 were increased in loaded animals at week one post-loading (3.6 ± 0.2) compared to non-loaded controls
157 (1.5 ± 0.2 , $CI=-3.02--1.18$). Following this initial inflammation, the maximum synovitis scores

158 progressively decreased with a mild inflammation still present at week three (2.6 ± 0.2) and no signs of
159 inflammation in loaded animals at week six post-loading (2 ± 0.4). Summed synovitis scores showed
160 the same trend, with synovitis being highest at week one and returning to normal at week six post-
161 loading. Contralateral knees showed no sign of synovial inflammation at any time point.

162

163 Corticosterone levels in the fur of mice collected post-mortem at each time point were analysed
164 (Fig.4). The results show increased corticosterone levels in loaded mice ($0.21\pm 0.04\text{ng/mg}$) compared
165 to non-loaded controls ($0.14\pm 0.01\text{ng/mg}$, $CI=-1.8--0.1$) one week post-loading. Later time points did
166 not show any differences between loaded mice and non-loaded controls.

167

168 The volume of both TH+ nerve fibres (Fig.5A) and CGRP+ nerve fibres (Fig.5B) remained
169 unchanged following MJL. Upon examination of the knee sections, it was evident that innervation
170 was most prevalent in the ligaments, menisci and periosteum. Other regions, like subchondral bone,
171 cartilage or synovial fluid did not consistently show any presence of nerves, see supplementary Fig2.
172 In all cases nerve density was higher in the ligaments compared to other compartments (Fig5C-H).
173 Images of TH+ and CGRP+ nerve fibres histology (Fig.6) illustrate the differences in morphology and
174 density between tissues. The profile of sympathetic and sensory nerve fibres was also different, with
175 TH+ nerve fibres showing a characteristic curling around blood vessels while CGRP+ nerves
176 typically having long, straight fibres.

177

178 The subchondral bone integrity, measured in the femur and tibia, did not show any changes between
179 loaded and non-loaded mice over time following MJL (Tab.1). Results were analysed per condyle
180 (data not shown) but this did not reveal any region-specific changes in subchondral bone integrity
181 following MJL.

182

183 Correlation analysis between pathology parameters and behavioural read-outs revealed that increasing
184 cartilage damage over time correlates significantly to an increased mechanical sensitivity following
185 MJL (Fig.7). The correlation analysis between pain behaviours and pathology parameters (cartilage
186 lesions, nerve volume, corticosterone levels, subchondral bone integrity and synovitis) at weeks one,
187 three and six post-loading is shown in Fig.7A. This analysis revealed that the maximum and summed
188 ipsilateral cartilage lesion severity following loading showed a consistent increasing positive
189 correlation to mechanical hypersensitivity and altered weight bearing as time progressed. Whilst the
190 other parameters measured did correlate to mechanical hypersensitivity at certain time points, these
191 did not show a pattern over time matching the MJL-induced progression of allodynia. In contrast, the
192 positive correlation between summed OA scores and ipsilateral mechanical threshold values increases
193 over time (Fig.7B) with significant interaction between time and ipsilateral mechanical difference
194 score on the summed OA scores ($p=0.0038$). Whilst there is no significant correlation present at

195 weeks one (correlation; 0.237, $p=0.4824$) and three (correlation; 0.478, $p=0.1368$) post-loading, this
196 does develop at week six post-loading (correlation; 0.729, $p=0.0072$). The calculated correlations and
197 corresponding p-values per parameter can be found in the supplementary data.

Journal Pre-proof

198 Discussion

199

200 We have previously shown that the mechanical joint loading can be used as an appropriate model to
201 measure OA-induced allodynia in mice [20]. Here we show that the increasing cartilage damage
202 following MJL matches the development of nociceptive behaviour, resulting in a positive correlation
203 between behavioural read-outs and severity of cartilage lesions six weeks post-loading. Furthermore,
204 we show that the other parameters of OA pathology measured did not show a clear pattern in their
205 correlation to the pain phenotype. The synovium showed signs of mild inflammation directly after
206 loading but this returned to normal as both cartilage lesions and nociceptive behaviour started to
207 develop. Likewise, stress levels, as indicated by fur corticosterone levels, are increased in the first
208 week following MJL but return to normal in weeks three and six post-loading. Bone integrity and
209 knee innervation were not altered by MJL. These findings provide a first step into understanding the
210 pain-structure relationship in the MJL model of knee OA.

211

212 MJL induces cartilage damage in the ipsilateral joint directly after loading whilst contralateral lesions
213 develop at a later stage. In accordance with literature [18, 20], these initial ipsilateral lesions induced
214 by the two-week loading regime progress and worsen over three weeks after which the severity of
215 cartilage damage stabilizes. Importantly, the time frame of lesion progression matches the
216 development of allodynia resulting in a positive correlation between cartilage damage and mechanical
217 hypersensitivity. Interestingly, onset of contralateral mechanical hypersensitivity also corresponds to
218 the development of cartilage damage. Contralateral behavioural and cartilage changes, however, are
219 only seen six weeks post-loading whereas ipsilateral changes occur from three weeks. This
220 contralateral phenotype could result from compensatory behaviour with ipsilateral allodynia inducing
221 altered gait and an overuse of the contralateral limb. Although these results suggest a role for cartilage
222 degradation in the development of OA-induced nociception, the combination of both ipsilateral and
223 contralateral phenotypes could also be indicative of central hypersensitization, comparable to that
224 seen in patients with OA [30]. Neuroplastic centralization of pain could, in part, explain the
225 disconnect seen between structural damage and pain severity [31] as centralized pain following OA
226 will also be present in the absence of structural damage [32]. Nevertheless, the link between cartilage
227 damage and nociceptive behaviour has been shown in both preclinical [33, 34] and clinical studies
228 [10, 31]. Driscoll et al. [35], showed that the severity of cartilage damage at the onset of nociception is
229 comparable in two different surgical models of OA; the destabilization of the medial meniscus
230 (DMM) and the partial meniscectomy (PMX) surgery. In the MJL model, the same severity of
231 cartilage damage is seen three weeks post-loading at onset of nociceptive behaviour. The link between
232 cartilage damage and pain is further supported by correlation studies that work to minimize between
233 patient confounding. These show that multiple measures for pain perception correlate to joint space
234 narrowing as a measure for cartilage degradation [12]. Together these results suggest that cartilage

235 damage could, at least in part, be responsible for both OA pain in patients and allodynia in animal
236 models of OA.

237

238 Further histological analysis of the synovial lining revealed that the initial signs of synovitis present
239 one week post-loading decrease at three weeks and are no longer present when nociceptive behaviour
240 is established at six weeks. Although osteoarthritis is generally thought to be non-inflammatory, it has
241 been suggested that subclinical synovitis may play a role in the early stages of OA [36]. Following the
242 MJL-induced trauma, debris from the degrading cartilage is released into the synovium and it is
243 possible that cells in the synovial membrane react to these pro-inflammatory mediators causing local
244 inflammation [37, 38] thus explaining the initial inflammation. These signs of inflammation, however,
245 decrease as the behavioural phenotype develops indicating that joint inflammation might not be
246 directly responsible for the allodynia seen in this model. This matches with surgical models of OA
247 pain where, after an initial inflammatory post-surgery phase, joint inflammation subsides whilst
248 nociceptive behaviour persists [39, 40]. Furthermore, there is no upregulation of inflammatory
249 markers in the joints of mice undergoing either DMM or PMX at the point of nociception onset [35].
250 Instead, in both *in vivo* and *in vitro* models, mechanically damaged chondrocytes produce pain-
251 sensitizing molecules like nerve growth factor, bradykinin receptors B1/B2, tachykinin, and
252 tachykinin receptor 1 [35]. The development of nociceptive behaviour following mechanical loading
253 further supports the suggestion that mechanical injury, rather than synovitis, could drive OA pain.

254

255 Corticosterone levels in the fur, as a measure for chronic stress were increased only in the first week
256 following loading. Exposure to stress results in the release of corticosteroids via the hypothalamic-
257 pituitary-adrenal-axis. These hormones ensure that sufficient energy is available and dampen the
258 immune function to enable a fight or flight reaction [41]. Elevated levels of corticosterone can
259 therefore be indicative of a stress reaction in rodents. In most cases these corticosteroids are measured
260 in either blood or saliva. The disadvantage of being the transient nature of the data with corticosteroid
261 levels reflecting only the hours or minutes preceding collection [42]. Corticosteroid hormones
262 released into the blood get incorporated into hair during growth and as such, post-mortem collected
263 hair can be used to evaluate chronic exposure to corticosteroids over time [43, 44]. The analysis of
264 corticosterone in the fur following MJL shows that mainly the loading period itself is stressful rather
265 than the chronic pain that develops at a later stage. It is, therefore, possible that the large variation
266 seen in behavioural readouts in the first week following MJL is due to the increased stress in loaded
267 animals.

268

269 Interestingly, joint innervation was not altered over time following MJL. Literature shows that intra-
270 articular injection of complement Freud's adjuvant (CFA), which induces painful joint inflammation,
271 leads to increased knee joint innervation and vascularization [28, 45]. This is supported by patient

272 data showing an increase in innervation and vascularization in subchondral bone, synovium and
273 menisci in painful knee OA [46, 47]. Results presented here show, to a large extent, the same
274 localization of TH+ sympathetic nerves and CGRP+ sensory nerve in ligaments, meniscus and
275 periosteum. Notably, both TH and CGRP staining was consistently low in the subchondral bone
276 compartment. This contradicts literature showing both innervation of bone [48] and an increase in
277 CGRP+ nerve fibres following surgical OA induction [49-52]. It has been shown that decalcification
278 of bone tissue reduces the immunoreactivity of the tissue [53] which could, in part, explain the
279 absence of subchondral bone innervation seen here. Furthermore, in contrast to the CFA model, knee
280 innervation is not increased following MJL. One explanation could be that, unlike the CFA model,
281 MJL does not cause severe joint inflammation and as such does not induce nerve sprouting.
282 Nevertheless, it is still possible that other MJL-induced neuronal changes are contributing to the
283 development of allodynia. In models of OA pain neuroplastic changes are typically seen at the level of
284 the dorsal root ganglia or spinal cord [54-57]. Additionally, there are reports showing that
285 sensitization to pain can be due to central sensitization [58, 59] or the recruitment of silent nociceptors
286 [60, 61], both processes that do not require a visible increase in joint innervation to induce
287 hypersensitivity. As such, more work needs to be done to fully understand the nature and extent of
288 neuronal contribution to MJL-induced nociception.

289

290 As with the joint innervation, MJL did not alter subchondral bone integrity. This contrasts with what
291 has been found in knee samples from OA patients showing that bone mineral density of the
292 subchondral bone increases as the cartilage volume decreases [62]. This cortical thickening as OA
293 pathology progresses also been reported in different murine OA models, including the MIA model
294 [63, 64], the DMM model [65, 66] and in the Str/Ort mice [67]. Using the MJL model we have not
295 been able to reproduce this subchondral bone phenotype. Accordingly, when this model was
296 originally characterized [18], changes in bone architecture were not seen in the ipsilateral knees of
297 mice loaded for two consecutive weeks at 9N. Instead cortical thickening was only visible following
298 five consecutive weeks of loading [19]. Possibly, the two-week loading regime used here was not
299 severe enough to induce clear changes in subchondral bone architecture. Furthermore, results show no
300 differences between loaded and non-loaded animals at individual time points indicating that loading at
301 9N does not induce an osteogenic effect. As the literature reports osteogenic effects with loading
302 regimes at 13N or higher [17], an osteogenic effect at 9N was not expected.

303

304 The correlation analysis revealed an increasing positive correlation between MJL-induced allodynia
305 and progressive cartilage damage over time. Interestingly, all other pathology markers measured did
306 not show a similar pattern in correlation to MJL-induced allodynia progression. Of note is that these
307 coefficients are dependent on the variation in the data. Groups and outcomes are, therefore, not
308 directly comparable. As mentioned previously, the pain-structure relationship in knee OA is

309 extremely complex and, whilst results presented add to our knowledge, much remains unknown
310 regarding other OA-related pathologies not measured here. Literature has demonstrated the
311 importance of tissue pathologies like bone marrow lesions [68] or meniscal pathology [69] in the
312 development of OA-associated pain; yet how these pathologies manifest themselves in the MJL model
313 and if they contribute to the behavioural phenotype is unknown. Although work remains to be done to
314 understand how cartilage damage induces nociceptive behaviour and which other tissue pathologies
315 potentially play in OA-associated pain, these findings provide valuable insight into the pain-structure
316 relationship in the MJL model.

Journal Pre-proof

317 **Acknowledgements**

318

319 This project has received funding from the European Union’s Horizon 2020 research and innovation
320 programme under the Marie Skłodowska-Curie grant agreement No 642720. Ana Paula Luiz is a
321 fellow of Versus Arthritis UK.

322

323 **Author contributions**

324

325 F. ter Heegde: Conception and design; collection and assembly of data; analysis and interpretation of
326 the data; drafting of the article; final approval of the article.

327 A.P. Luiz: Administrative, technical, or logistic support; collection and assembly of data.

328 S. Santana-Varela: Administrative, technical, or logistic support; collection and assembly of data

329 R. Magnusdottir: Conception and design; analysis and interpretation of the data

330 M. Hopkins: Administrative, technical, or logistic support; analysis and interpretation of the data

331 Y. Chang: Conception and design; analysis and interpretation of the data

332 B. Poulet: Administrative, technical, or logistic support; analysis and interpretation of the data

333 R. Fowkes: Administrative, technical, or logistic support; analysis and interpretation of the data; final
334 approval of the article

335 J.N.Wood: Critical revision of the article for important intellectual content; obtaining of funding; final
336 approval of the article.

337 C. Chenu: Conception and design; critical revision of the article for important intellectual content;
338 obtaining of funding; final approval of the article

339

340 **Role of funding source**

341

342 The funders had no role in study design, data collection and analysis, decision to publish, or
343 preparation of the manuscript.

344

345 **Conflict of interest**

346

347 None of the authors have any conflict of interest to disclose

348 **References**

349

- 350 1. Martel-Pelletier, J., et al., *Osteoarthritis*. Nat Rev Dis Primers, 2016. **2**: p. 16072.
- 351 2. O'Neill, T.W. and D.T. Felson, *Mechanisms of Osteoarthritis (OA) Pain*. Curr Osteoporos
352 Rep, 2018. **16**(5): p. 611-616.
- 353 3. Torres, L., et al., *The relationship between specific tissue lesions and pain severity in persons
354 with knee osteoarthritis*. Osteoarthritis Cartilage, 2006. **14**(10): p. 1033-40.
- 355 4. Lo, G.H., et al., *Strong association of MRI meniscal derangement and bone marrow lesions in
356 knee osteoarthritis: data from the osteoarthritis initiative*. Osteoarthritis Cartilage, 2009.
357 **17**(6): p. 743-7.
- 358 5. Felson, D.T., et al., *The association of bone marrow lesions with pain in knee osteoarthritis*.
359 Ann Intern Med, 2001. **134**(7): p. 541-9.
- 360 6. Sowers, M.F., et al., *Magnetic resonance-detected subchondral bone marrow and cartilage
361 defect characteristics associated with pain and X-ray-defined knee osteoarthritis*.
362 Osteoarthritis Cartilage, 2003. **11**(6): p. 387-93.
- 363 7. Hunter, D.J., et al., *The reliability of a new scoring system for knee osteoarthritis MRI and the
364 validity of bone marrow lesion assessment: BLOKS (Boston Leeds Osteoarthritis Knee
365 Score)*. Ann Rheum Dis, 2008. **67**(2): p. 206-11.
- 366 8. Hill, C.L., et al., *Knee effusions, popliteal cysts, and synovial thickening: association with
367 knee pain in osteoarthritis*. J Rheumatol, 2001. **28**(6): p. 1330-7.
- 368 9. Kornaat, P.R., et al., *Osteoarthritis of the knee: association between clinical features and MR
369 imaging findings*. Radiology, 2006. **239**(3): p. 811-7.
- 370 10. Link, T.M., et al., *Osteoarthritis: MR imaging findings in different stages of disease and
371 correlation with clinical findings*. Radiology, 2003. **226**(2): p. 373-81.
- 372 11. Wluka, A.E., et al., *How does tibial cartilage volume relate to symptoms in subjects with knee
373 osteoarthritis?* Ann Rheum Dis, 2004. **63**(3): p. 264-8.
- 374 12. Neogi, T., et al., *Association between radiographic features of knee osteoarthritis and pain:
375 results from two cohort studies*. BMJ, 2009. **339**: p. b2844.
- 376 13. Hill, C.L., et al., *Synovitis detected on magnetic resonance imaging and its relation to pain
377 and cartilage loss in knee osteoarthritis*. Ann Rheum Dis, 2007. **66**(12): p. 1599-603.
- 378 14. Pelletier, J.P., et al., *A new non-invasive method to assess synovitis severity in relation to
379 symptoms and cartilage volume loss in knee osteoarthritis patients using MRI*. Osteoarthritis
380 Cartilage, 2008. **16 Suppl 3**: p. S8-13.
- 381 15. Englund, M., et al., *Incidental meniscal findings on knee MRI in middle-aged and elderly
382 persons*. N Engl J Med, 2008. **359**(11): p. 1108-15.
- 383 16. Bhattacharyya, T., et al., *The clinical importance of meniscal tears demonstrated by magnetic
384 resonance imaging in osteoarthritis of the knee*. J Bone Joint Surg Am, 2003. **85-A**(1): p. 4-9.
- 385 17. De Souza, R.L., et al., *Non-invasive axial loading of mouse tibiae increases cortical bone
386 formation and modifies trabecular organization: a new model to study cortical and
387 cancellous compartments in a single loaded element*. Bone, 2005. **37**(6): p. 810-8.
- 388 18. Poulet, B., et al., *Characterizing a novel and adjustable noninvasive murine joint loading
389 model*. Arthritis Rheum, 2011. **63**(1): p. 137-47.
- 390 19. Poulet, B., et al., *Intermittent applied mechanical loading induces subchondral bone
391 thickening that may be intensified locally by contiguous articular cartilage lesions*.
392 Osteoarthritis Cartilage, 2015. **23**(6): p. 940-8.
- 393 20. Ter Heegde, F., et al., *Non-invasive mechanical joint loading as an alternative model for
394 osteoarthritic pain*. Arthritis Rheumatol, 2019.
- 395 21. Chaplan, S.R., et al., *Quantitative assessment of tactile allodynia in the rat paw*. J Neurosci
396 Methods, 1994. **53**(1): p. 55-63.
- 397 22. Malfait, A.M., C.B. Little, and J.J. McDougall, *A commentary on modelling osteoarthritis
398 pain in small animals*. Osteoarthritis Cartilage, 2013. **21**(9): p. 1316-26.
- 399 23. Piel, M.J., J.S. Kroin, and H.J. Im, *Assessment of knee joint pain in experimental rodent
400 models of osteoarthritis*. Methods Mol Biol, 2015. **1226**: p. 175-81.

- 401 24. Piel, M.J., et al., *Pain assessment in animal models of osteoarthritis*. Gene, 2014. **537**(2): p. 184-8.
- 402
- 403 25. Kuyinu, E.L., et al., *Animal models of osteoarthritis: classification, update, and measurement of outcomes*. J Orthop Surg Res, 2016. **11**: p. 19.
- 404
- 405 26. Glasson, S.S., et al., *The OARSI histopathology initiative - recommendations for histological assessments of osteoarthritis in the mouse*. Osteoarthritis Cartilage, 2010. **18 Suppl 3**: p. S17-23.
- 406
- 407
- 408 27. Lewis, J.S., et al., *Acute joint pathology and synovial inflammation is associated with increased intra-articular fracture severity in the mouse knee*. Osteoarthritis Cartilage, 2011. **19**(7): p. 864-73.
- 409
- 410
- 411 28. Jimenez-Andrade, J.M. and P.W. Mantyh, *Sensory and sympathetic nerve fibers undergo sprouting and neuroma formation in the painful arthritic joint of geriatric mice*. Arthritis Res Ther, 2012. **14**(3): p. R101.
- 412
- 413
- 414 29. Chartier, S.R., et al., *Exuberant sprouting of sensory and sympathetic nerve fibers in nonhealed bone fractures and the generation and maintenance of chronic skeletal pain*. Pain, 2014. **155**(11): p. 2323-36.
- 415
- 416
- 417 30. Lluch, E., et al., *Evidence for central sensitization in patients with osteoarthritis pain: a systematic literature review*. Eur J Pain, 2014. **18**(10): p. 1367-75.
- 418
- 419 31. Pelletier, J.P., et al., *Risk factors associated with the loss of cartilage volume on weight-bearing areas in knee osteoarthritis patients assessed by quantitative magnetic resonance imaging: a longitudinal study*. Arthritis Res Ther, 2007. **9**(4): p. R74.
- 420
- 421
- 422 32. Finan, P.H., et al., *Discordance between pain and radiographic severity in knee osteoarthritis: findings from quantitative sensory testing of central sensitization*. Arthritis Rheum, 2013. **65**(2): p. 363-72.
- 423
- 424
- 425 33. Nwosu, L.N., et al., *Relationship between structural pathology and pain behaviour in a model of osteoarthritis (OA)*. Osteoarthritis Cartilage, 2016. **24**(11): p. 1910-1917.
- 426
- 427 34. Tran, P.B., et al., *Spinal microglial activation in a murine surgical model of knee osteoarthritis*. Osteoarthritis Cartilage, 2017. **25**(5): p. 718-726.
- 428
- 429 35. Driscoll, C., et al., *Nociceptive Sensitizers Are Regulated in Damaged Joint Tissues, Including Articular Cartilage, When Osteoarthritic Mice Display Pain Behavior*. Arthritis Rheumatol, 2016. **68**(4): p. 857-67.
- 430
- 431
- 432 36. Mathiessen, A. and P.G. Conaghan, *Synovitis in osteoarthritis: current understanding with therapeutic implications*. Arthritis Res Ther, 2017. **19**(1): p. 18.
- 433
- 434 37. de Lange-Brokaar, B.J., et al., *Synovial inflammation, immune cells and their cytokines in osteoarthritis: a review*. Osteoarthritis Cartilage, 2012. **20**(12): p. 1484-99.
- 435
- 436 38. Sokolove, J. and C.M. Lepus, *Role of inflammation in the pathogenesis of osteoarthritis: latest findings and interpretations*. Ther Adv Musculoskelet Dis, 2013. **5**(2): p. 77-94.
- 437
- 438 39. Knights, C.B., C. Gentry, and S. Bevan, *Partial medial meniscectomy produces osteoarthritis pain-related behaviour in female C57BL/6 mice*. Pain, 2012. **153**(2): p. 281-92.
- 439
- 440 40. Inglis, J.J., et al., *Regulation of pain sensitivity in experimental osteoarthritis by the endogenous peripheral opioid system*. Arthritis Rheum, 2008. **58**(10): p. 3110-9.
- 441
- 442 41. de Kloet, E.R., M. Joels, and F. Holsboer, *Stress and the brain: from adaptation to disease*. Nat Rev Neurosci, 2005. **6**(6): p. 463-75.
- 443
- 444 42. Hellhammer, J., et al., *Several daily measurements are necessary to reliably assess the cortisol rise after awakening: state- and trait components*. Psychoneuroendocrinology, 2007. **32**(1): p. 80-6.
- 445
- 446
- 447 43. Pragst, F. and M.A. Balikova, *State of the art in hair analysis for detection of drug and alcohol abuse*. Clin Chim Acta, 2006. **370**(1-2): p. 17-49.
- 448
- 449 44. Erickson, R.L., C.A. Browne, and I. Lucki, *Hair corticosterone measurement in mouse models of type 1 and type 2 diabetes mellitus*. Physiol Behav, 2017. **178**: p. 166-171.
- 450
- 451 45. Ghilardi, J.R., et al., *Neuroplasticity of sensory and sympathetic nerve fibers in a mouse model of a painful arthritic joint*. Arthritis Rheum, 2012. **64**(7): p. 2223-32.
- 452
- 453 46. Eitner, A., et al., *The innervation of synovium of human osteoarthritic joints in comparison with normal rat and sheep synovium*. Osteoarthritis Cartilage, 2013. **21**(9): p. 1383-91.
- 454

- 455 47. Ashraf, S., et al., *Increased vascular penetration and nerve growth in the meniscus: a*
456 *potential source of pain in osteoarthritis*. *Ann Rheum Dis*, 2011. **70**(3): p. 523-9.
- 457 48. Serre, C.M., et al., *Evidence for a dense and intimate innervation of the bone tissue, including*
458 *glutamate-containing fibers*. *Bone*, 1999. **25**(6): p. 623-9.
- 459 49. Zhu, S., et al., *Subchondral bone osteoclasts induce sensory innervation and osteoarthritis*
460 *pain*. *J Clin Invest*, 2019. **129**(3): p. 1076-1093.
- 461 50. Shao, Y.J., et al., *Sensory nerves protect from the progression of early stage osteoarthritis in*
462 *mice*. *Connect Tissue Res*, 2019: p. 1-11.
- 463 51. Aso, K., et al., *Nociceptive phenotype alterations of dorsal root ganglia neurons innervating*
464 *the subchondral bone in osteoarthritic rat knee joints*. *Osteoarthritis Cartilage*, 2016. **24**(9): p.
465 1596-603.
- 466 52. Obeidat, A.M., et al., *The nociceptive innervation of the normal and osteoarthritic mouse*
467 *knee*. *Osteoarthritis Cartilage*, 2019.
- 468 53. Chartier, S.R., et al., *Immunohistochemical localization of nerve growth factor, tropomyosin*
469 *receptor kinase A, and p75 in the bone and articular cartilage of the mouse femur*. *Mol Pain*,
470 2017. **13**: p. 1744806917745465.
- 471 54. Otis, C., et al., *Spinal neuropeptide modulation, functional assessment and cartilage lesions*
472 *in a monosodium iodoacetate rat model of osteoarthritis*. *Neuropeptides*, 2017. **65**: p. 56-62.
- 473 55. Ogbonna, A.C., et al., *Pain-like behaviour and spinal changes in the monosodium iodoacetate*
474 *model of osteoarthritis in C57Bl/6 mice*. *Eur J Pain*, 2013. **17**(4): p. 514-26.
- 475 56. Orita, S., et al., *Pain-related sensory innervation in monoiodoacetate-induced osteoarthritis*
476 *in rat knees that gradually develops neuronal injury in addition to inflammatory pain*. *BMC*
477 *Musculoskelet Disord*, 2011. **12**: p. 134.
- 478 57. Miller, R.E., et al., *Visualization of Peripheral Neuron Sensitization in a Surgical Mouse*
479 *Model of Osteoarthritis by In Vivo Calcium Imaging*. *Arthritis Rheumatol*, 2018. **70**(1): p. 88-
480 97.
- 481 58. Harvey, V.L. and A.H. Dickenson, *Behavioural and electrophysiological characterisation of*
482 *experimentally induced osteoarthritis and neuropathy in C57Bl/6 mice*. *Mol Pain*, 2009. **5**: p.
483 18.
- 484 59. Schuelert, N. and J.J. McDougall, *Grading of monosodium iodoacetate-induced osteoarthritis*
485 *reveals a concentration-dependent sensitization of nociceptors in the knee joint of the rat*.
486 *Neurosci Lett*, 2009. **465**(2): p. 184-8.
- 487 60. Prato, V., et al., *Functional and Molecular Characterization of Mechanoinsensitive "Silent"*
488 *Nociceptors*. *Cell Rep*, 2017. **21**(11): p. 3102-3115.
- 489 61. Hirth, M., et al., *Nerve growth factor induces sensitization of nociceptors without evidence for*
490 *increased intraepidermal nerve fiber density*. *Pain*, 2013. **154**(11): p. 2500-11.
- 491 62. Bobinac, D., et al., *Changes in articular cartilage and subchondral bone histomorphometry in*
492 *osteoarthritic knee joints in humans*. *Bone*, 2003. **32**(3): p. 284-90.
- 493 63. Mohan, G., et al., *Application of in vivo micro-computed tomography in the temporal*
494 *characterisation of subchondral bone architecture in a rat model of low-dose monosodium*
495 *iodoacetate-induced osteoarthritis*. *Arthritis Res Ther*, 2011. **13**(6): p. R210.
- 496 64. Boudenot, A., et al., *Effect of interval-training exercise on subchondral bone in a chemically-*
497 *induced osteoarthritis model*. *Osteoarthritis Cartilage*, 2014. **22**(8): p. 1176-85.
- 498 65. Iijima, H., et al., *Effects of short-term gentle treadmill walking on subchondral bone in a rat*
499 *model of instability-induced osteoarthritis*. *Osteoarthritis Cartilage*, 2015. **23**(9): p. 1563-74.
- 500 66. Das Neves Borges, P., T.L. Vincent, and M. Marenzana, *Automated assessment of bone*
501 *changes in cross-sectional micro-CT studies of murine experimental osteoarthritis*. *PLoS*
502 *One*, 2017. **12**(3): p. e0174294.
- 503 67. Stok, K.S., et al., *Revealing the interplay of bone and cartilage in osteoarthritis through*
504 *multimodal imaging of murine joints*. *Bone*, 2009. **45**(3): p. 414-22.
- 505 68. Foong, Y.C., et al., *The clinical significance, natural history and predictors of bone marrow*
506 *lesion change over eight years*. *Arthritis Res Ther*, 2014. **16**(4): p. R149.
- 507 69. Roubille, C., et al., *The presence of meniscal lesions is a strong predictor of neuropathic pain*
508 *in symptomatic knee osteoarthritis: a cross-sectional pilot study*. *Arthritis Res Ther*, 2014.
509 **16**(6): p. 507.

Figure legends**Figure 1: Development of mechanical hypersensitivity and altered weight bearing following MJL**

The right knees of mice were loaded three times per week for two weeks at 9N (red line, $n = 12$ per time point) to induce OA. Behavioural read-outs were compared to non-loaded isoflurane controls (black dotted line, $n = 12$ per time point). Mice were sacrificed at weeks one (**A, D, G**), three (**B, E, H**) and six (**C, F, I**) post-loading. Development of mechanical hypersensitivity was measured using von Frey filaments (50% paw withdrawal threshold (PWT) in grams) in the ipsilateral (**A, B, C**) and contralateral (**D, E, F**) paws. Altered weight bearing (weight placed on ipsilateral paw as a percentage of total weight placed on both legs) was measured using the incapacitance test (**G, H, I**). Differences between non-loaded and loaded animals are indicated with # ($p < 0.05$), ## ($p < 0.01$) or ### ($p < 0.001$) whilst a change within groups over time (compared to baseline value) are indicated with a * ($p < 0.05$), ** ($p < 0.01$) or *** ($p < 0.001$) in corresponding colours. Values given as the mean \pm SD.

Figure 2: Severity of OA-like cartilage lesions following MJL

Ipsilateral and contralateral knees of 9N-loaded mice (red squares, $n = 5-6$) were collected post mortem at weeks one, three and six post-loading after which OA severity was scored for each joint section. Values were compared to non-loaded isoflurane controls (black circles, $n = 5-6$). Scoring system ranges from 0-6, OA severity is classified as either low (grade 0-2), mild (grade 3-4) or severe (grade 5-6). For each sample, maximum scores (**A**; ipsilateral knees, **B**; contralateral knees), determined as the lesions with the highest severity, and summed scores (**C**; ipsilateral knees, **D**; contralateral knees) are given. Differences in the severity of OA lesions between groups are indicated with a * ($p < 0.05$), ** ($p < 0.01$) or *** ($p < 0.001$). Values given as mean \pm SD. Representative images of toluidine blue stained, coronal knee sections are shown for the ipsilateral knee at one (**E**), three (**F**) and six (**G**) weeks post-loading as for the contralateral knee at one (**H**), three (**I**) and six (**J**) weeks post-loading. Yellow arrows indicate damage to the cartilage that was scored as OA-like. Images shown are 25x magnification with scale bars representing 200 μ m

Figure 3: Severity of synovitis following MJL

Ipsilateral and contralateral knees of 9N-loaded mice (red squares, $n = 5-6$) were collected post mortem at weeks one, three and six post-loading after which the severity of synovitis was scored for each joint section. Values were compared to non-loaded isoflurane controls (black circles, $n = 5-6$). Scoring system ranges from 0-6, synovitis is classified as either low (grade 0-2), mild (grade 3-4) or severe (grade 5-6). For each sample, maximum (**A**; ipsilateral knees, **B**; contralateral knees) and summed scores (**C**; ipsilateral knees, **D**; contralateral knees) are given. Differences in the severity of synovitis between groups are indicated with a * ($p < 0.05$), ** ($p < 0.01$) or *** ($p < 0.001$). Values given as mean \pm SD.

38 Figure 4: Corticosterone levels in the fur of loaded and non-loaded mice after MJL

39 Fur of 9N-loaded mice (red squares, $n = 6$) and non-loaded isoflurane controls (black circles, $n = 6$)
40 were collected post mortem at weeks one, three and six post-loading. The fur was processed and
41 analysed to determine the corticosterone levels as a measure for chronic stress. Differences in
42 corticosterone levels are indicated with a * ($p < 0.05$). Values given as mean \pm SD.

43

44 Figure 5: Tyrosine hydroxylase (TH) and calcitonin gene-related peptide (CGRP) positive nerve
45 fibres following MJL

46 Ipsilateral knees of 9N-loaded mice (red squares, $n = 5$) and non-loaded isoflurane controls (black
47 circles, $n = 5$) were collected post mortem at weeks one, three and six post-loading. Knees were
48 processed for nerve analysis after which the total volume of TH+ (A) and CGRP+ (B) nerve fibres
49 were determined. There were no significant differences in total nerve volumes. Innervation of TH+
50 (C, E, F) and CGRP+ (D, F, H) nerve fibres in the respective compartments; lateral meniscus (LM),
51 medial meniscus (MM), cruciate ligament (CM), the lateral collateral ligament (LCL), medial
52 collateral ligament (MCL), and periosteum (P), is given as a volume at week one (C, D), three (E, F)
53 and six (H, I) weeks post-loading. Values given as mean \pm SD.

54

55 Figure 6: Visualization of TH+ and CGRP+ labelling in specified regions of the knee joint of loaded
56 and non-loaded mice at week one following MJL

57 Innervation of the knee joint was imaged in coronal sections (A). Regions used to image are showed
58 on toluidine blue stained section (B). Examples of typical nerve fibres expressing TH+ (C) and
59 CGRP+ (D) are shown for the lateral collateral ligament, medial collateral ligament, cruciate
60 ligament, lateral meniscus, medial meniscus and periosteum of loaded and non-loaded ipsilateral
61 knees at week one post-loading. Images are shown at 40x magnification with scale bars representing
62 50 μ m.

63

64 Figure 7: Correlation analysis between pain behaviours and OA parameters following MJL

65 Overall correlation analysis (A) was run between parameters for OA-like severity of cartilage damage
66 (green), nerve volume (violet), corticosterone levels (red), subchondral bone integrity (purple) or
67 synovitis scoring (yellow) and nociceptive behaviour at weeks one, three and six post-loading. For
68 each time point, differences between baseline and final behavioural thresholds (difference score) of
69 the ipsilateral mechanical thresholds (50% PWT) and weight bearing values (% weight ipsilateral)
70 were used as behavioural read-outs for the correlation analysis. Correlations range from -1 (dark blue;
71 indicative of perfect negative correlation) to 1 (dark red; indicative of perfect positive correlation).
72 Specific correlation between ipsilateral mechanical threshold difference scores plotted against the
73 summed OA cartilage scores (B) is shown for loaded mice and non-loaded controls sacrificed at

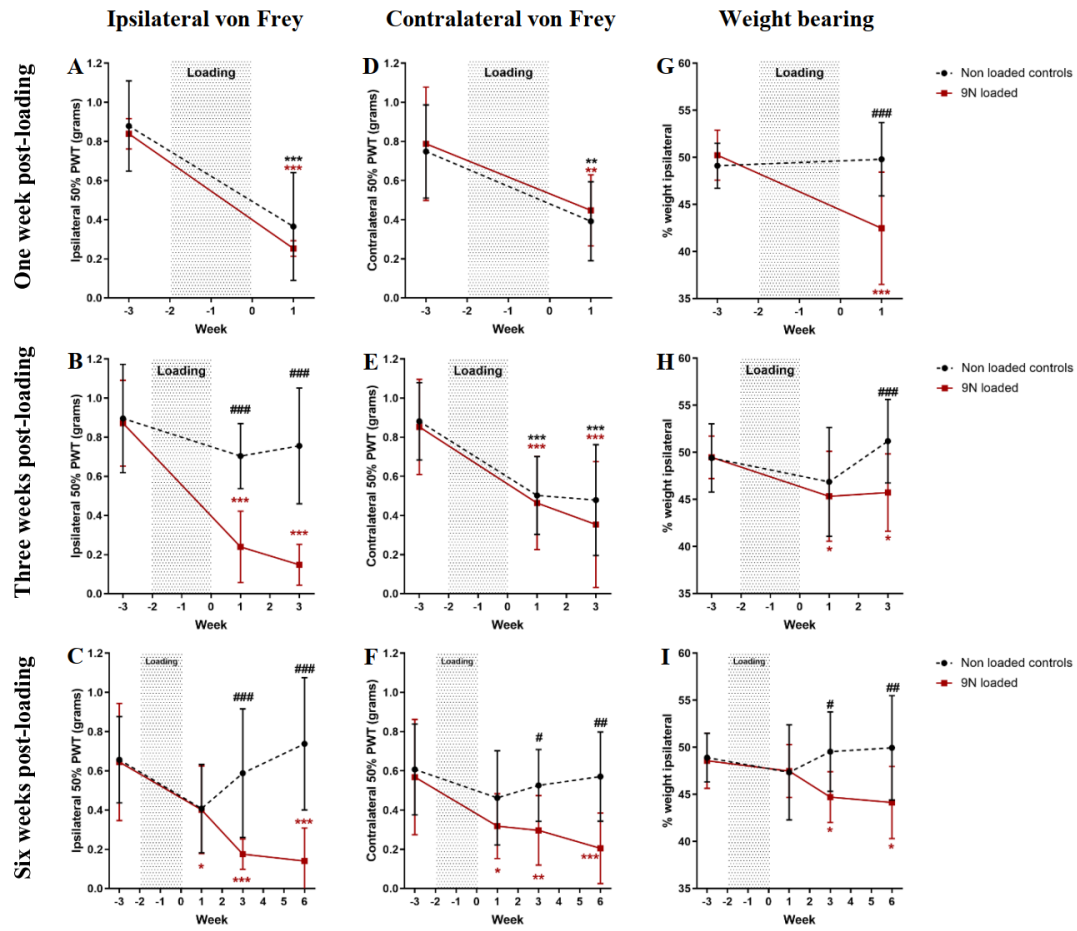
- 74 weeks one (orange dots, $n = 11$), three (blue dots, $n = 11$) and six (green dots, $n = 12$) post-loading.
- 75 Linear trendlines and corresponding R2 values are portrayed on the graph.

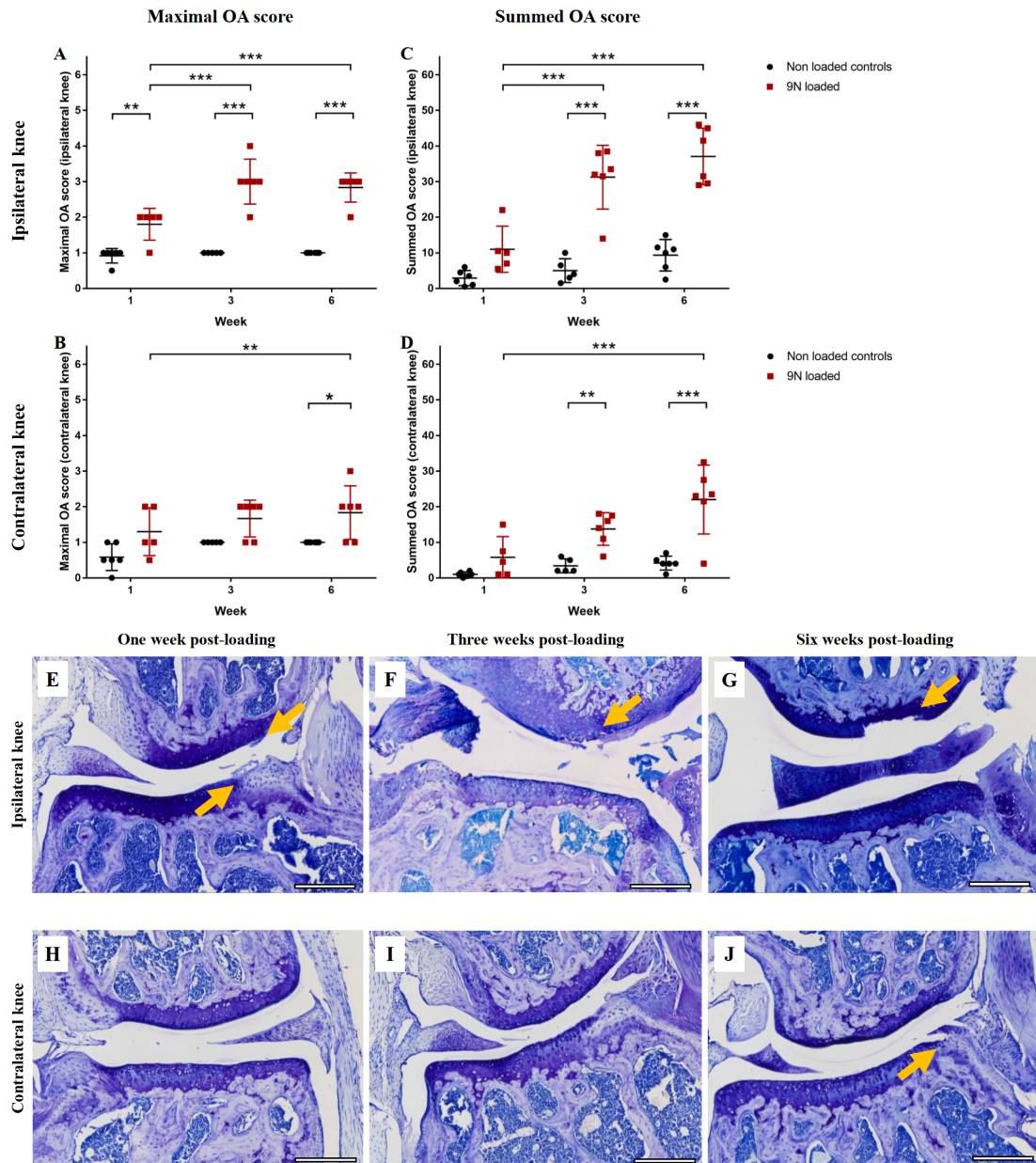
Journal Pre-proof

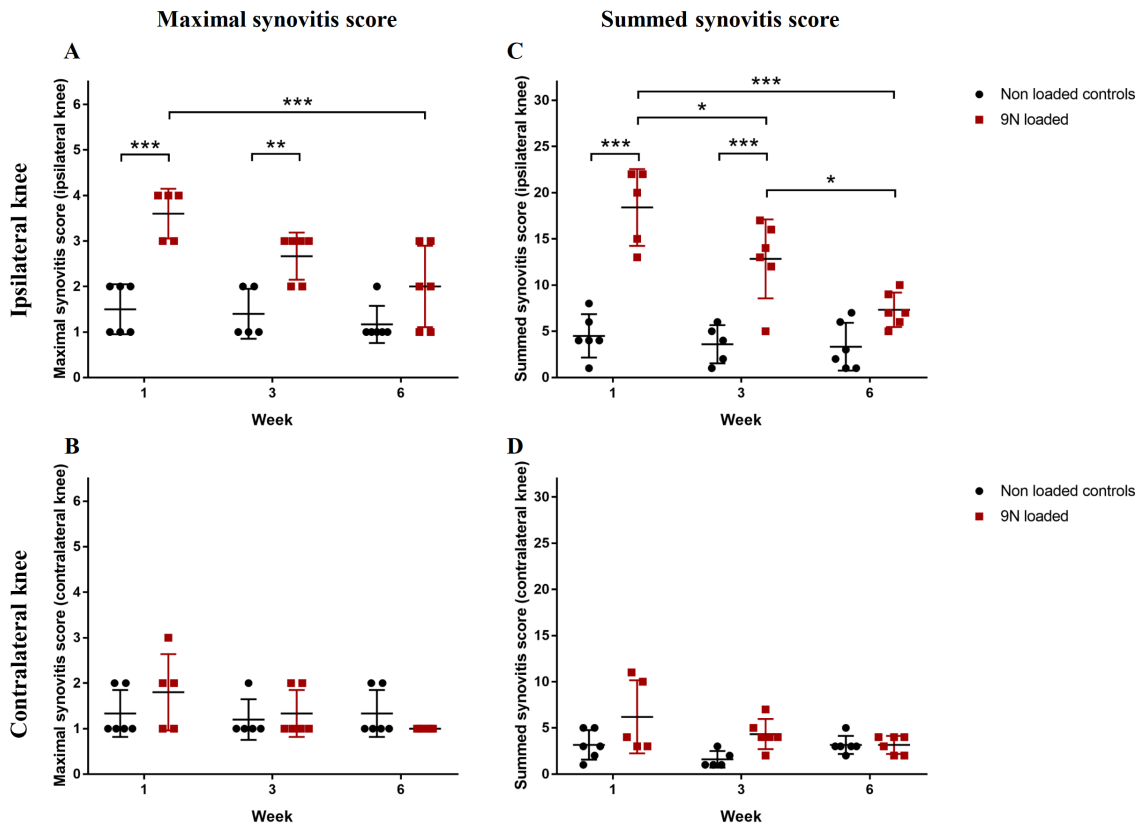
Table 1 Summary μ CT parameters of subchondral bone in loaded and non-loaded mice following MJL

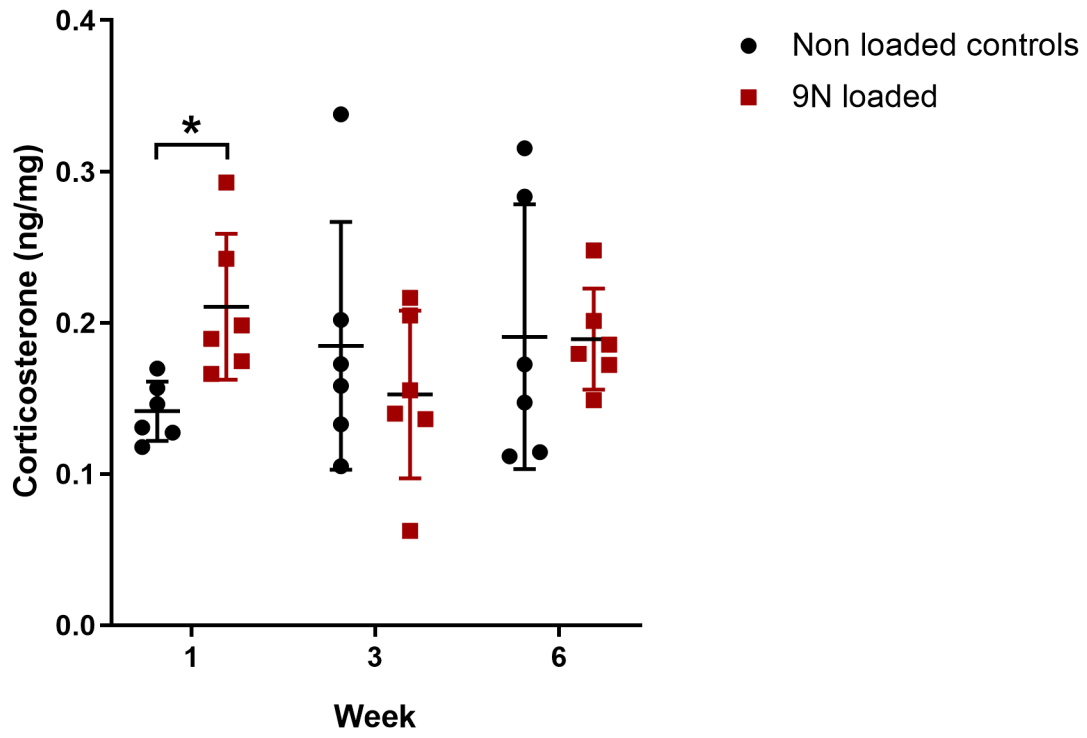
There were no significant differences in μ CT parameters between non-loaded controls and loaded mice. Values given as mean \pm SEM with corresponding p -values.

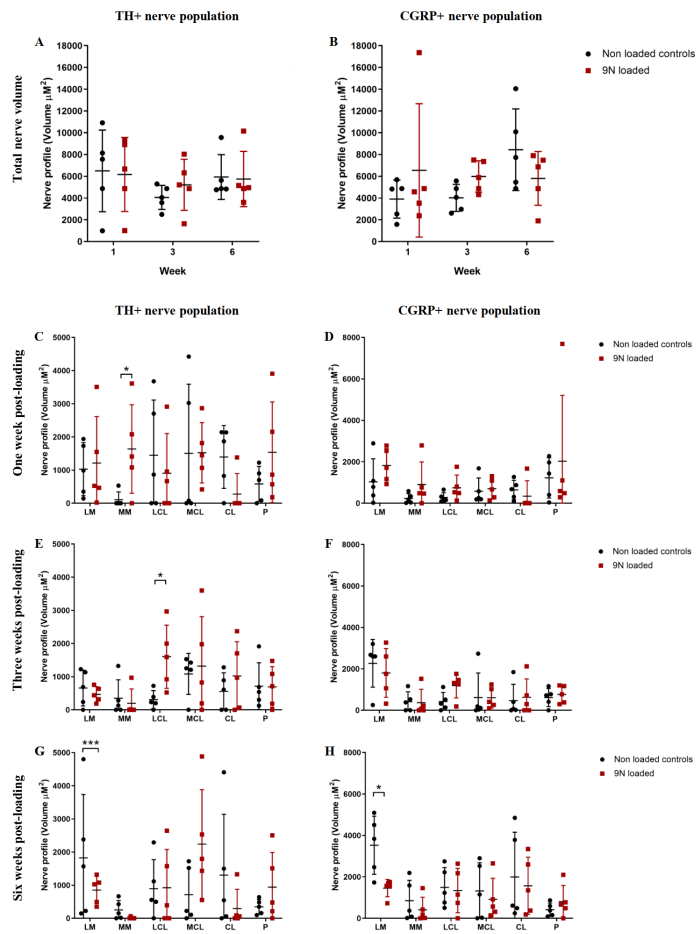
μ CT Parameter	Region of interest	Condition	One week post-loading	Three weeks post-loading	Six weeks post-loading
subchondral plate thickness (mm)	Tibia	Non-loaded control	0.052 \pm 0.001	0.084 \pm 0.002	0.095 \pm 0.002
		Loaded	0.052 \pm 0.001	0.087 \pm 0.001	0.098 \pm 0.003
		p - value	> 0.9999	0.7641	0.6570
	Femur	Non-loaded control	0.083 \pm 0.002	0.075 \pm 0.002	0.083 \pm 0.002
		Loaded	0.083 \pm 0.002	0.077 \pm 0.001	0.088 \pm 0.003
		p - value	0.9912	0.9513	0.1632
Trabecular BV/TV (%)	Tibia	Non-loaded control	43.12 \pm 1.34	40.06 \pm 1.87	46.77 \pm 1.51
		Loaded	47.26 \pm 1.85	44.98 \pm 1.10	43.79 \pm 2.09
		p - value	0.2271	0.1453	0.4997
	Femur	Non-loaded control	43.55 \pm 1.48	40.44 \pm 1.66	46.95 \pm 0.94
		Loaded	45.17 \pm 1.09	43.55 \pm 1.28	44.68 \pm 1.90
		p - value	0.8031	0.3733	0.5930
Trabecular thickness (mm)	Tibia	Non-loaded control	0.051 \pm 0.002	0.050 \pm 0.002	0.058 \pm 0.001
		Loaded	0.054 \pm 0.002	0.055 \pm 0.002	0.056 \pm 0.002
		p - value	0.3583	0.1313	0.6610
	Femur	Non-loaded control	0.054 \pm 0.002	0.053 \pm 0.002	0.062 \pm 0.001
		Loaded	0.056 \pm 0.001	0.057 \pm 0.002	0.059 \pm 0.003
		p - value	0.8462	0.4034	0.6191

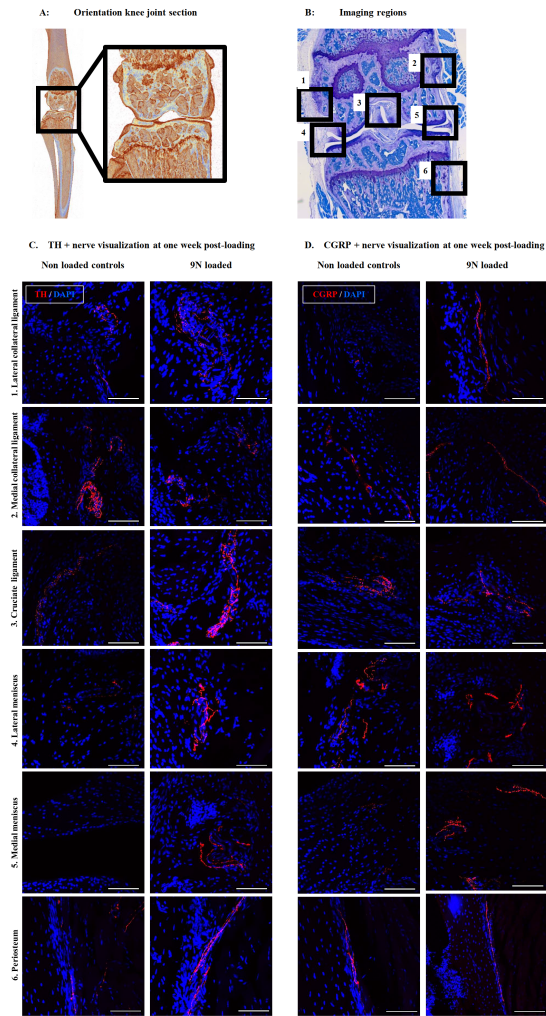




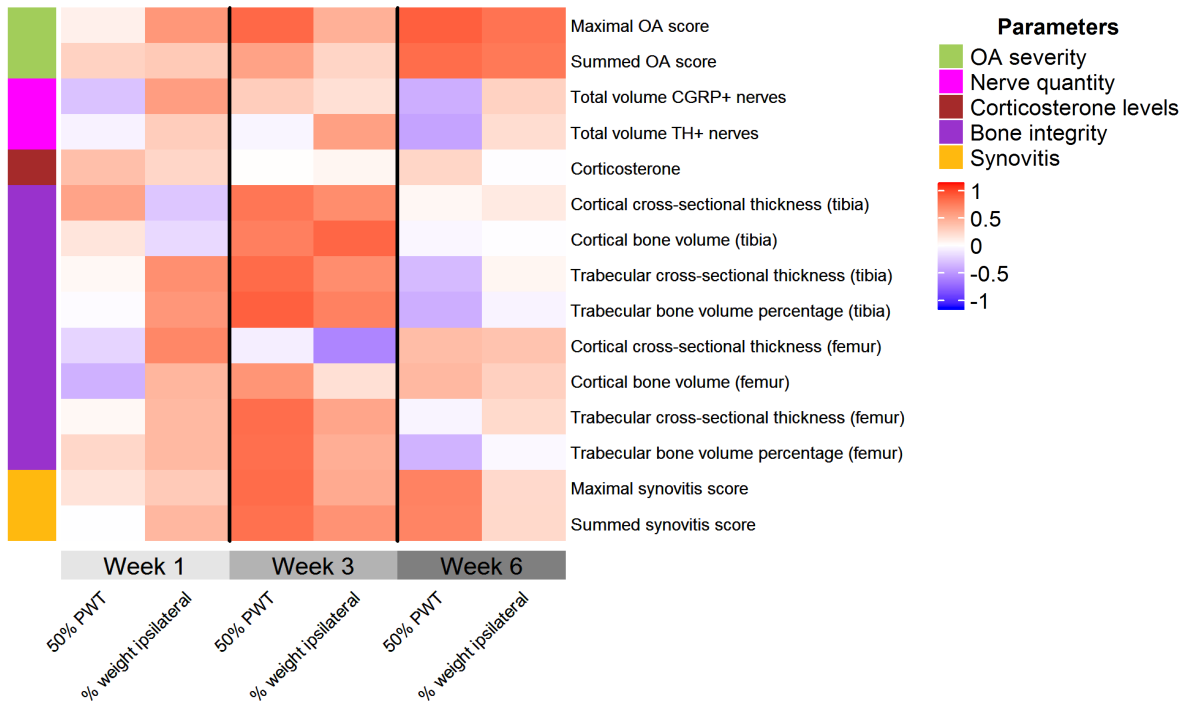








A. Overall correlation analysis between behavioural and pathological parameters



B. Correlation between summed OA score and ipsilateral mechanical hypersensitivity

